are skeptical of this result for two reasons. First, on 6 February and 23 March the increasing flux (longitude increases with time) was observed as Io set in the west. The high brightness was obtained at high air mass and could be an artifact due to incorrectly estimating the extinction. Second, the initial analysis of the speckle measurements does not show the signature of a hot spot as should be the case. One or more possible minor hot spots on the leading side may have elevated the overall flux by 5 to 10% (20 to 40 GW μm^{-1} str^{-1}). There was no sign of major activity at any longitude.

These observations provide a detailed picture of Io's volcanism before and after the Ulysses encounter. Volcanic thermal emission from Io was at the low end of the normal range at all Io longitudes during this period. Activity at Loki, normally the dominant hot spot, was at a low level, and no other major outbursts were seen. This sustained volcanically quiet period should provide a test of any mechanisms expected to deliver atoms from volcanic eruptions to the magnetosphere on time scales of less than a few months, as particles from such sources should have been depleted in the magnetosphere at the time of the Ulysses encounter. For comparison, Voyager 1 observed a 4.8-μm vertical flux of 93 GW μm^{-1} str^{-1} from Loki (9), a factor of 2.5 greater than the value on 24 January 1992 (Table 2).

REFERENCES AND NOTES

1. D. B. Nash, M. H. Carr, J. Gradie, D. M. Hunten, C. F. Yoder, in *Satellites*, J Burns and M. Matthews, Eds. (Univ. of Arizona Press, Tucson), pp 629–688 (1986).
2. R. R. Howell and W. M. Sinton, in *Proceedings of the Workshop on Time-Variable Phenomena in the Jovian System*, M. Belton, R. West, J. Rahe, Eds. Lowell Observatory, Flagstaff, AZ, 25 to 27 August 1987 (*NASA SP-494*, National Aeronautics and Space Administration (NASA), Washington, DC, 1989), pp. 47–62.
3. N. M. Schneider, W. H. Smyth, M. A. McGrath, in *ibid.*, pp. 75–99.
4. W. M. Sinton and C. Kaminski, *Icarus* **75**, 207 (1988).
5. W M. Sinton *et al.*, *Astron. J.* **96**, 1095 (1988).
6 J. R. Spencer *et al.*, *Nature* **348**, 618 (1990)
7. J. R. Spencer, unpublished material.
8. W. H. Press, B. P. Flannery, S. A. Teukolsky, W. T. Vettering, *Numerical Recipes* (Cambridge Univ. Press, Cambridge, 1986).
9. J. C Pearl and W. M Sinton, in *Satellites of Jupiter*, D. Morrison, Ed (Univ of Arizona Press, Tucson, 1982), pp 724–755.
10. A. S. McEwen, N. R. Isbell, J. C. Pearl, *Lunar Planet. Sci.* **XXIII**, 881 (1992).
11. R. R. Howell and M. T. McGinn, *Science* **230**, 63 (1985).
12. W. M. Sinton, D. Lindwall, F. Cheigh, W. C. Tittemore, *Icarus* **54**, 133 (1983).

13. The work was funded by NASA Planetary Astronomy grants NAGW-2785 and NAGW-1276. J.R.S., B.E.C., and D.O. performed the work at the IRTF; R.R.H. and D.R.K. performed the observations in Wyoming. We thank K. Kuntz for the use of his simplex algorithm.

1 June 1992; accepted 3 August 1992

Imaging Observations of Jupiter's Sodium Magneto-Nebula During the Ulysses Encounter

Michael Mendillo, Brian Flynn, Jeffrey Baumgardner

Jupiter's great sodium nebula represents the largest visible structure traversed by the Ulysses spacecraft during its encounter with the planet in February 1992. Ground-based imaging conducted on Mount Haleakala, Hawaii, revealed a nebula that extended to at least ±300 Jovian radii (spanning ~50 million kilometers); it was somewhat smaller in scale and less bright than previously observed. Analysis of observations and results of modeling studies suggest reduced volcanic activity on the moon Io, higher ion temperatures in the plasma torus, lower total plasma content in the torus, and fast neutral atomic clouds along the Ulysses inbound trajectory through the magnetosphere. Far fewer neutrals were encountered by the spacecraft along its postencounter, out-of-ecliptic trajectory.

The detection of a vast cloud of sodium gas extending from Jupiter into interplanetary space (*1*) has prompted a reexamination of the complex processes that govern atmospheric-magnetospheric interactions in the Jovian system (*2–5*). Neutral sodium atoms are a relatively minor component of Jupiter's environment, but their strong light-scattering efficiency makes them an ideal "tracer" for processes that are otherwise often difficult to observe. As summarized recently (*6*), the sodium chain begins with volcanic sources on Jupiter's moon Io that deposit sodium on its surface and in its atmosphere. These atoms are subsequently liberated by sputtering processes driven by the energetic particles in Jupiter's strong magnetosphere. The resultant cloud of gaseous sodium orbits Jupiter near Io (*7*). Energetic electrons in this region collisionally ionize sodium with a characteristic time (1 to 4 hours) that is far shorter than the solar extreme ultraviolet (EUV) ionization time constant (400 hours). Thus, Na^+ is added as a trace species to the plasma torus that surrounds Jupiter (*8*). These Na^+ ions are quickly accelerated by the rapidly rotating magnetic field to a velocity of 74 km/s. Collisions with the more abundant torus population results in a thermalized distribution of Na^+ that is characteristic of the torus as a whole.

The vast sodium nebula that extends to ±500 Jovian radii (R_J) is composed of streaming Na atoms that are ejected from the vicinity of Io at speeds well above escape speed. The sources of these fast sodium atoms (Na*) are far from certain. Resonant charge exchange between corotating Na^+ in the torus and orbital Na near Io

$$Na^+ + Na \rightarrow Na^+ + Na^* \qquad (1)$$

was suggested (*2*) and has been the basis of modeling studies (*4*, *5*). Recently, the dissociation of a Na–molecular ion source has been proposed as a mechanism for producing Na* (*3*). Because there are no appreciable sources or sinks for Na* throughout the magnetosphere beyond Io, observations of the resultant sodium nebula can be used as a remote sensing diagnostic for the magnetospheric plasma processes in the source region. Hence, the term "magneto-nebula" is used to describe a structure intimately tied to magnetospheric physics.

A ground-based imaging campaign was organized (*9*) to set the initial context for the in situ particle and field observations made by the Ulysses instruments. However, the remote-sensing observations also predict, constrain, and enhance results from the spacecraft-based studies. Consequently, two widely separated sites were selected for ground-based coordination of magneto-nebula imaging for several days spanning the encounter date (8 February 1992). At the Mount Haleakala Observatory on Maui, Hawaii, excellent data sets were obtained from 5 through 11 February 1992.

Boston University, Center for Space Physics, 725 Commonwealth Avenue, Boston, MA 02215.

Table 1. Comparison of observed and derived sodium magneto-nebula parameters.

Observation period	Brightness at 100 R_J (rayleighs)	Flare angle (deg)	Na* source requirements (10^{26} atoms per second)	Torus ion energy (eV)
November to December 1989	75	21 ± 4	10	85
January 1990	25	21 ± 3	3	85
Ulysses encounter February 1992	10	27 ± 5	2	135

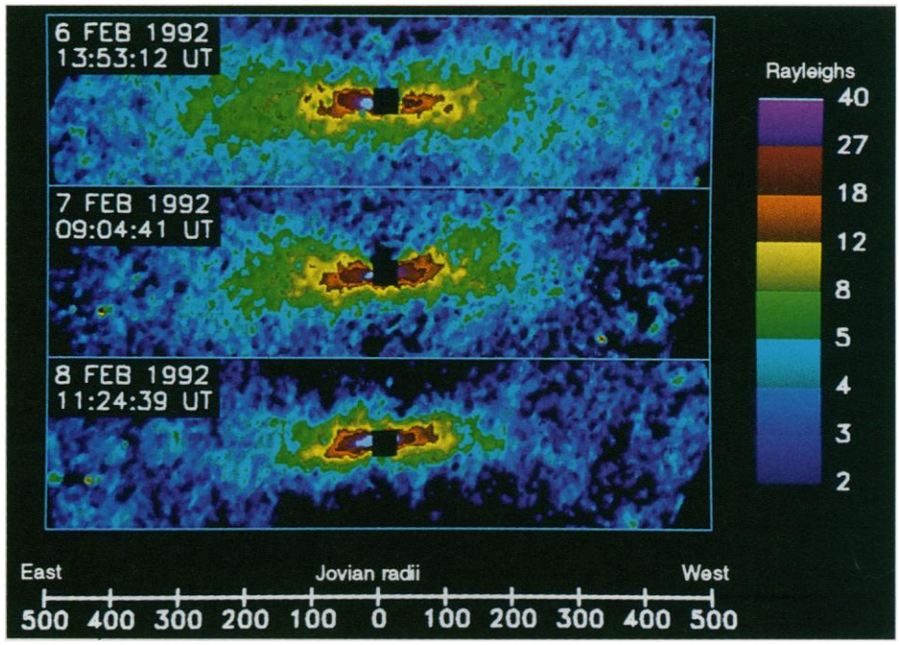

Fig. 1. Images of combined D1 + D2 sodium emission from Mount Haleakala Observatory during days preceding Ulysses closest approach to Jupiter on 8 February 1992. Times refer to the beginning of an image acquisition sequence that lasts for ~30 min. The dark square results from an occulting mask corresponding to ±10 R_J used to block light from Jupiter and Io.

At the McDonald Observatory in Fort Davis, Texas, image sets were obtained on 6, 8, and 10 February. In this report we confine our analysis to the observations from Haleakala.

The instrumentation developed for imaging studies of extended planetary signatures consists of a 4-inch refractor with narrowband interference filters and an image-intensified charge-coupled device (CCD) detector (*1*, *5*). The observational technique involves the use of on- and off-target images at sodium and control wavelengths, with standard image processing and calibration procedures (*1*, *5*).

As with previous data sets, the sodium nebula for the Ulysses inbound encounter period is seen as an elongated structure spanning the equatorial plane; it extends far beyond magnetospheric boundaries (100 to 150 R_J) (Fig. 1). Intensities during the Ulysses flyby, however, were the lowest yet observed (Table 1). North-south image scans at various radial distances show that the intensity profile is approximately Gaussian, with a half-width at half-maximum that increases linearly with distance from the planet, resulting in a flaring of the nebula with respect to the Jovian equatorial plane (*1*, *5*). During the Ulysses encounter period, this flaring was noticeably the largest we have observed (Table 1). With the use of absolute intensity calibration and the observed flaring angle, one can estimate the source rate for fast sodium S(Na*) (*10*). As suggested by the low intensity levels, S(Na*) for the Ulysses period was also the lowest yet observed.

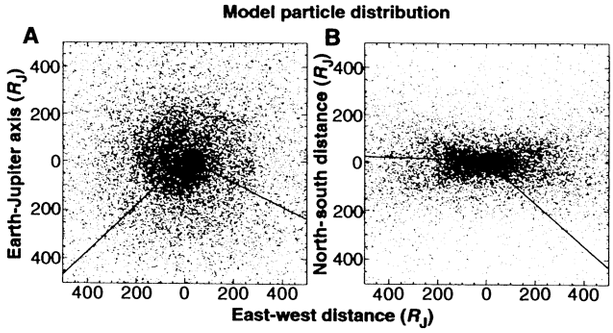

Fig. 2. Particle distributions resulting from the charge-exchange model (*5*) for combined fast- and slow-speed sodium atoms adjusted to yield the average intensities and nebula flaring angle in Fig. 1. (**A**) View from north of the equatorial plane. (**B**) View from Earth. The solid line indicates the Ulysses spacecraft trajectory through the modeled particle distribution.

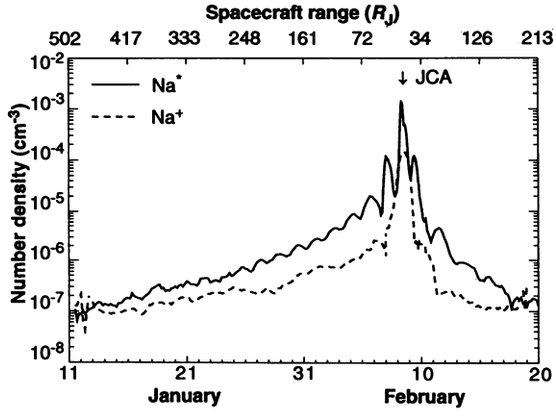

Fig. 3. Sodium atom volume density versus time along the equivalent Ulysses trajectory through the particle distributions given in Fig. 2. The structure along the inbound trajectory results from spiral arm structures in the model nebula. Results from the outbound trajectory also show some spiral structure, with a rapid decrease in Na densities as the spacecraft dips below the Jovian equatorial plane. The dashed line profile shows where solar EUV-produced Na^+ appears along the trajectory. The relatively high proportions of ions within 50 R_J result from photo-ionization of the slower speed Na components of the charge-exchange model (*4*, *5*), which are not given sufficient energy to escape Jupiter when ejected from Io's orbit. JCA, Jupiter closest approach.

In addition to helping define the source rate, the flaring angle, can be related directly to conditions in the plasma torus. Within the framework of the resonant charge exchange model given by Eq. 1, sodium atoms are ejected with the corotation speed (V_{co} = 74 km/s) at Io's orbital distance. This velocity is directed parallel to the Jovian equatorial plane and perpendicular to the local radius vector. In addition to V_{co}, there is a randomly oriented component with a Maxwellian distribution corresponding to the thermal speed (V_{th}) of the corotating Na^+ just before charge exchange (*1*, *11*). If the velocity-space distribution of ions in the torus is assumed to be spherical about the corotation speed, the radius of the sphere is given by

$$V_{th} = V_{co} \sin \theta \qquad (2)$$

For the images shown in Fig. 1, $\theta = 27°$, and thus V_{th} = 34 km/s. When converted to kinetic energy, the ion population in the torus is thus determined to be 135 eV, the highest ion temperature so inferred to date. Because the ions are cooled by collisions with electrons (with energy subsequently radiated), the derived higher ion energy could result from reduced cooling. Such a case would imply that the plasma densities

were low (that is, fewer Coulomb collisions) in the torus (*12*, *13*). Alternatively, the spatial relation between the cool and hot components of the plasma torus and Io's sodium cloud might have changed. As a result, more neutral particles would encounter hot ions. Table 1 summarizes the full set of observational and model-derived quantities.

The three-dimensional distribution of the Na* volume density required to match an image can be modeled within the charge-exchange framework discussed above (*4*, *5*) (Fig. 2). The Ulysses trajectory through the modeled particle distribution can be used to specify the [Na*] density at the spacecraft's location (Fig. 3). For simulation runs with and without photo-ionization, there is a slight difference between the [Na*] distributions; these are designated [Na^+] in Fig. 3. It should be noted that Na^+ can appear by other means (*14*). Moreover, the Na^+ energy should be higher than the 600 eV associated with corotational escape from Io's location because of capture by the rapidly rotating magnetic field at larger distances. Nevertheless, the simulations depicted in Fig. 3 should give a good prediction for fast neutral clouds (Na* is a tracer for other gases). In the absence of significant radial transport, the simulations also provide a rough estimate of where ions produced by solar EUV might appear. Scaling of this latter effect to gases other than sodium would require the use of their respective solar ionizing time constants in the simulation.

In summary, ground-based imaging observations of Jupiter's great sodium nebula during the Ulysses encounter period indicated that (i) volcanic activity on Io preceding the Ulysses encounter must have been lower than observed in 1989 to 1990; (ii) plasma torus densities derived from the neutrals were proportionally lower; and (iii) the ion thermal structure in the torus was higher than in previous years.

REFERENCES AND NOTES

1. M. Mendillo *et al.*, *Nature* **348**, 312 (1990).
2. A. Eviatar, Y. Mekler, and F. V. Coroniti [*Astrophys. J.* **205**, 662 (1976)] predicted a flux of hot (fast) neutral sodium that was subsequently observed and treated in detail by R. Brown and N. Schneider [*Icarus* **48**, 519 (1981)].
3. N. M. Schneider *et al.*, *Science* **253**, 1394 (1991).
4. W. Smyth and M. Combi, *J. Geophys. Res.* **96**, 22711 (1991).
5. B. Flynn, M. Mendillo, J. Baumgardner, *Icarus*, in press.
6. N. Schneider, W. Smyth, M. McGrath, in *Time-Variable Phenomena in the Jovian System*, M. Belton, R. West, J. Rahe, Eds. [National Aeronautics and Space Administration (NASA), Washington, DC, 1989], pp. 75–94.
7. Io is located at 5.9 R_J, where the orbital speed is 17.3 km/s. The corotation speed at 5.9 R_J is 74 km/s.
8. The dominant ion species in the plasma torus are O^+, S^+, and S^{2+}. See review by F. Bagenal, in *Time-Variable Phenomena in the Jovian System*, M. Belton, R. West, J. Rahe, Eds. (NASA, Washington, DC, 1989), pp. 196–210.
9. N. Schneider, *Eos* **73**, 173 (1992).
10. With the approximations that all Na* is confined within the flaring angle and that the nebula is azimuthally symmetric, the source rate becomes $S(Na^*) = 4\pi r^2 \sin\theta\, V_{term} n$, where r is the distance from Jupiter, θ is the flaring angle, V_{term} is the terminal flow speed (70 km/s), and $n = N_\tau/\pi r$ is the volume density at r in the equatorial plane [N_τ is the sodium line of sight column content derived from the observed emission intensity ϵ in Rayleighs ($\epsilon = 0.48 \times 10^{-6} N_\tau$)] (*5*).
11. A. F. Cheng [*J. Geophys. Res.* **91**, 4524 (1986)] and D. D. Barbosa and A. Eviatar [*Astrophys. J.* **310**, 927 (1986)] were the first to discuss this nonradial velocity component that leads to the flaring angle.
12. Ion cooling is discussed by D. D. Barbosa, F. V. Coroniti, and A. Eviatar [*Astrophys. J.* **274**, 429 (1983)] and is reviewed recently by A. F. Cheng [*Adv. Space Res.* **12**, 353 (1992)].
13. As discussed in E. J. Smith, K.-P. Wenzel, and D. F. Page [*Science* **257**, 1503 (1992)], most of the Ulysses instruments were turned off during the period of torus passage in order to safeguard their use for the primary mission. Indications of lower plasma densities in the torus were obtained by the radio beacon experiment (M. K. Bird *et al.*, *ibid.*, p. 1531).
14. Ions created from a "magnetospheric neutral wind" by photo-ionization and their subsequent radial transport are discussed in A. Eviatar and D. D. Barbosa [*J. Geophys. Res.* **89**, 7393 (1984)] and D. D. Barbosa [*ibid.* **91**, 5605 (1986)].

15. We thank N. Schneider for coordination of the Jupiter Watch Campaign; E. Smith for providing Ulysses trajectory information; D. Nottingham for assisting in the observations and data analysis; and D. Barbosa for informative discussions. We thank the director and staff of the Mount Haleakala Observatory for their assistance. This work was funded, in part, by NASA grant NAGW-2679.

29 May 1992; accepted 31 July 1992

Hubble Space Telescope Imaging of the North Polar Aurora on Jupiter

J. Caldwell, B. Turgeon, X.-M. Hua

The first direct images of the Jovian aurora at ultraviolet wavelengths were obtained by the Hubble Space Telescope Faint Object Camera near the time of the Ulysses spacecraft encounter with Jupiter on 8 February 1992. The auroral oval is not uniformly luminous. It exhibits a brightness minimum in the vicinity of longitude 180°. In the few images available, the brightest part of the oval occurs in late afternoon Jovian time. The observed oval is not concentric with calculated ovals in the O_6 model of Connerney. The size of the oval is consistent with auroral particles on field lines with magnetic *L* parameter >8, indicating significant migration from Io, its torus, or both, if these are their origins.

An aurora is the visible interaction between a planet's magnetosphere and its atmosphere. Auroral observations provide information on planetary magnetic fields (and thus, planetary interiors), magnetospheric species, and atmospheric composition and dynamics. Previous ultraviolet (UV) observations of the Jovian aurora from spacecraft such as the International Ultraviolet Explorer (IUE) and the Voyagers were made with spectrographs with large apertures and permitted only indirect inferences of spatial characteristics. Ground-based infrared (IR) images have also been obtained, but they are somewhat degraded spatially by Earth's atmosphere. We present here UV images of the Jovian aurora obtained by the Hubble Space Telescope (HST) that reveal the auroral oval for the first time. The images generally confirm previous auroral observations and models of the Jovian magnetic field, with some significant exceptions.

The HST Faint Object Camera (FOC) obtained six images (Fig. 1) of the Jovian north polar aurora in the H_2 Lyman band near 160-nm wavelength. The images were taken in two groups of three (Table 1), respectively ~13 and 3 hours before the time of closest approach to Jupiter by the Ulysses spacecraft (*1*, *2*).

The photometric properties of Jupiter enhance the observability of its aurora (*3*). Increased absorption of UV sunlight at the poles (Fig. 1) due to high-latitude, high-altitude aerosols provides a relatively dark background. If the background at the poles were as bright as at lower latitudes, auroral contrast would be greatly reduced.

Images 101, 102, and 201 have similar central meridian longitudes (CMLs) in System III (*4*) (~150°) and images 202 and 203 also have similar CMLs (~190°). In each H_2 image an auroral oval may be seen, with those at CML ~190° having more favorable orientations. For each case, the astronomically westernmost part of the oval (local Jovian evening) is the brightest, with a second brightness maximum at the easternmost position.

Limb brightening, which occurs in an optically thin emitting region, is not the primary determinant of the apparent brightness variations along the oval. First, it could not introduce the observed east-west

Space Astrophysics Laboratory, Institute for Space and Terrestrial Science, 2700 Steeles Avenue West, Suite 202, Concord, ON L4K 3C8, Canada.